Solar Energy Materials and Solar Cells 171 (2017) 187–196

Contents lists available at ScienceDirect

Solar Energy Materials and Solar Cells

journal homepage: www.elsevier.com/locate/solmat

Experimental and numerical investigation of AA6082-T6 thin plates welding using Concentrated Solar Energy (CSE)

D.I. Pantelis[a], P.N. Karakizis[a,*], M.E. Kazasidis[a], D.G. Karalis[b], J. Rodrıguez[c]

[a] Shipbuilding Technology Laboratory, School of Naval Architecture and Marine Engineering, National Technical University of Athens, 9 Heroon, Polytechniou st., Zografos, Athens GR-157 80, Greece

[b] Hellenic Navy, Hellenic Naval Academy, Mechanics and Materials Division, Marine Materials Laboratory, Hazjikyriakou Avenue, Piraeus 185 39, Greece

[c] CIEMAT – Plataforma Solar de Almería, Aptdo. 22, E-04200 Tabernas, Almería, Spain

ARTICLE INFO

Keywords:
Concentrated solar energy
Aluminum
Welding
Scanning electron microscopy
Microhardness
Tensile testing
Finite element analysis
Thermal modeling

ABSTRACT

In the present study Concentrated Solar Energy (CSE) was used in order to weld thin plates (3 mm thickness) of the 6082 aluminum alloy in the T6 condition. A specially designed vacuum chamber and a cooling system were utilized in order to create the inert atmosphere and the heat dissipation required, respectively. The experiments resulted in the production of a sound butt weld between the aluminum plates which presented a 23% and 32% reduction of the microhardness and the Ultimate Tensile Strength (UTS) respectively compared to the base metal but are in good correlation with other fusion welding methods of the same material. Finally, based on the experimental results, a finite element 3D thermal model of the process was developed that can be used for the design and optimization of welds of aluminum alloys using the same experimental set-up.

1. Introduction

A lot of attention has been devoted in the last two decades in Concentrated Solar Energy (CSE) research. CSE is provided from an unlimited energy source, the sun, making it a very energy efficient and environmentally friendly treatment method that is why several solar facilities have been placed in different locations with very high levels of sunshine all year round. Despite the fact that it is not yet efficient to construct an industrial facility for CSE thermal processing of metallic materials, a lot of research has been conducted on the subject. Initially, CSE has been mostly used as a surface heat treatment method. Vazquez et al. [1], Rodriguez et al. [2–6], and Yang et al. [7] achieved the hardening of steels by thermally treating them using CSE. Later, a lot more surface treatments have been examined such as cladding [8–10], nitriding [11,12] and SHS coatings [13].

Romero et al. [14] focused on the welding of H13 tool steel and AISI 316 L stainless steel plates of various thicknesses and geometrical configurations under argon protective atmosphere. Full penetration beads without any defects were produced for both materials by optimizing the tracking speed, solar radiation and geometrical configuration for all the different joint configurations such as flush corner, single-V butt and T-joints. In addition, the same research team achieved Ti6Al4V titanium alloy welding using concentrated solar energy [15]. They used 5 mm thick plates in a flush corner joint configuration. The solar radiation was very high (1000 W/cm^2) and the welding speed very low (0.15 mm/s). Although an increase in the grain size in the heat affected zones is observed, the microhardness is close to the equivalent of the base material throughout the entire welded piece.

Concerning the welding of aluminum alloys using CSE, a few publications exist in the international literature. Karalis et al. [16] triggered the research on this topic in 2005. Their research focused on bead on block and plate on block experiments using aluminum and specifically the AA7075-T6. Although plate on block welding was only partially achieved, a lot of observations and conclusions were drawn concerning the penetration depth as well as the microstructure, microhardness and metallurgical transformations during the process. Despite the fact that aluminum was also the material of choice for Cambronero et al. [17], their research focused on metal foam joining. They used an aluminum-silicon alloy as a filler between aluminum foam plates. The CSE melted and foamed the filler which joined the plates together, even in a non-protective atmosphere.

To the best of the authors' knowledge there is no study in the international literature describing proper CSE welding of aluminum plates. In the present study the authors achieved sound welding of thin AA6082-T6 plates using CSE. The use of both a vacuum chamber in order to create inert atmosphere and a specially designed cooling system was mandatory. The microstructure, microhardness and mechanical properties of the weld were studied. Finally, based on the

* Corresponding author.
E-mail address: karakizisp@gmail.com (P.N. Karakizis).

http://dx.doi.org/10.1016/j.solmat.2017.06.063
Received 9 May 2017; Received in revised form 27 June 2017; Accepted 28 June 2017

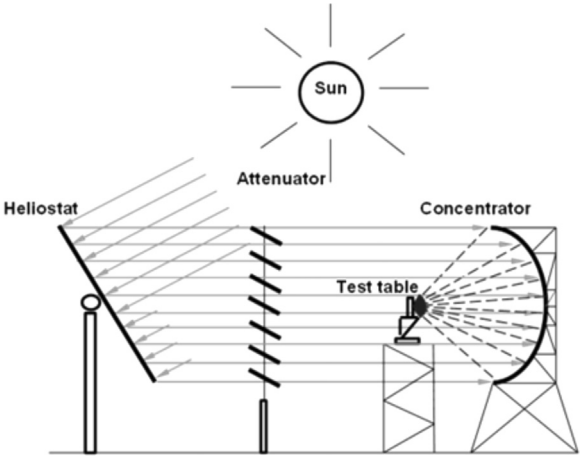

Fig. 1. Schematic diagram of the solar furnace SF40 installation of the PSA.

experimental results, a finite element model of the process was developed.

2. Experimental procedure

The experiments were carried out utilizing the high concentration solar furnace SF40 at the Plataforma Solar de Almeria (PSA) in Spain. As it can be observed in Fig. 1 the operating principle of the solar furnace is the following. The heliostat which reflects the sun has a flat area of 100 m^2. It reflects the sun rays, via the attenuator which consists of large metallic shutters, to the parabolic concentrator which has a projecting area of 56.5 m^2. It should be mentioned at this point that the heliostat automatically tracks the sun during the day and that the maximum flux achieved is 7000 kW/m^2 in a focus with a diameter of 12 cm. Afterwards, the focused sun beam is directed to a tilted mirror in order to switch from the horizontal to the vertical plane.

Plates of AA6082 in the T6 tempering condition were used in the procedure. The plates with dimensions of 100 × 50 × 3 mm^3 were butt welded and the nominal chemical composition of the plate material is presented in Table 1.

The sides of the plates were in full contact without any machining such as a bevel. They were grinded and cleaned with ethanol and the upper surfaces were sprayed with graphite in order to reduce the surface reflectivity of the aluminum. A 5 mm wide graphite layer was applied at each plate resulting in a total 10 mm width as it can be observed in Fig. 2a. The rest of the upper surface of the plates was covered with thin zirconia sheets in order to be insulated from the CSE as it can be observed in Fig. 2b. An inert gas (pure argon) atmosphere was mandatory in order to prevent the oxidation of the molten aluminum and hence a vacuum chamber had to be used as it can be observed in Fig. 2c. The active cooling system depicted in Fig. 2d was made of two hollow stainless steel plates with running water at room temperature flowing through them.

The variables of the experiment were the following. The solar irradiation (W/m^2) which was solely defined by the weather, the traverse speed represented as the percentage of the maximum achievable speed and the percentage of the attenuator shutter opening with 0% representing fully closed shutters and 100% fully open. Because the solar irradiation was variable the authors chose to conduct most of the experiments with the slowest speed possible (1% i.e. 0.648 mm/s) and 100% shutter opening. Five experiments were conducted by altering only the irradiation within a range from 784 to 943 W/m^2. Finally, after these trials, a sound weld was achieved by the mean 893 W/m^2 irradiation value.

After the welding process the sound weld was cut at transverse sections regarding to the welding direction and the appropriate metallographic preparation took place. After grinding and polishing the specimens were etched for around 4 s using the “modified Poulton's reagent”. Afterwards the macroscopic observation was conducted using a Leica MZ6 optical stereoscope, a Leica DMILM optical microscope and a Jeol 6390LV scanning electron microscope equipped with an Oxford Instruments Inca energy 250 Energy Dispersive Spectroscopy system. In addition, the microhardness distribution was measured using a Wolpert Wilson 402MVD microhardness tester with a load of 3 N and a dwelling time of 10 s. Finally, an MTS hydraulic mechanical testing machine of 100 kN maximum load was used in order to realize the tensile tests. The elongation was measured using an MTS ± 10 mm extensometer and the deformation speed was 0.25 mm/min.

3. Results and discussion

3.1. Microstructural characterization

The as received welded plates are presented in Fig. 3a. It can be observed that the extent of the molten zone differs slightly throughout the length of the weld as it is wider in the middle as well as the trailing edge. This can be attributed to the small alternation of the solar irradiation during the experiment as every experiment conducted with 1% traverse speed took several minutes to be completed. As a result the authors decided to make three transverse sections for the metallographic observation of the specimens. In Fig. 3b these three distinct transverse sections are presented, No 1 at x = 18 mm, No 2 at x = 45 mm and No 3 at x = 60 mm. Notice that start of welding was realized at the right edge of the welded plates (x = 0 mm).

Optical stereoscope images of the three transverse sections after polishing and etching are presented in Fig. 4. Because there are no substantial differences concerning the microstructure and the appearance between the three sections, the rest of the observation is going to be conducted on the No 1 section (which is presented in Fig. 4a) in order to avoid unnecessary repetitions. The fusion zone morphology resembles the equivalent that occurs after other fusion welding methods such as that of the Gas Tungsten Arc Welded [18,19] and the Modified Indirect Electric Arc Welded AA6082 [20]. In addition, the fusion zone has a typical trapezoid shape being narrower at the bottom surface which was in contact with the cooling system and as a result was cooled down faster. It should be mentioned that a small drop in thickness by around 0.5 mm from the top surface can be observed, something that was expected due to the lack of filler material. The average width of the upper side of the molten zone is 18.40 ± 1.03 mm while the equivalent of the bottom side is 16.74 ± 1.23 mm.

In Fig. 5 typical optical micrographs at 100× magnification are presented from the areas presented with arrows in Fig. 5c. First, it should be mentioned that no porosity is observed. As melting of the material occurs, during solidification further cooling of the molten material in the center of the Fusion Zone (FZ) results in the formation of smaller equiaxed grains with an average diameter of 0.25 mm due to the reduced supercooling in this zone (see Fig. 5a). As the cooling of the molten material continues, the grains grow in the direction opposite to the direction of the heat flow i.e. perpendicular to the liquid-solid

Table 1
Chemical composition of the AA6082-T6 (wt%).

Si	Fe	Cu	Mn	Mg	Cr	Zn	Ti	Ni	Ga	V	Al
1.07	0.28	0.04	0.7	1.15	0.024	0.04	0.015	0.005	0.013	0.016	Bal.